PSMD8 Promotes Breast Cancer Progression and Attenuates Paclitaxel Sensitivity by Regulating the Expression of KIF10

Zhiyu Li
Renmin Hospital of Wuhan University: Wuhan University Renmin Hospital
Chenyuan Li
Renmin Hospital of Wuhan University: Wuhan University Renmin Hospital
Yi Tu
Renmin Hospital of Wuhan University: Wuhan University Renmin Hospital
Feng Yao
Renmin Hospital of Wuhan University: Wuhan University Renmin Hospital
Shengrong Sun
Renmin Hospital of Wuhan University: Wuhan University Renmin Hospital
Shichong Liao
Renmin Hospital of Wuhan University: Wuhan University Renmin Hospital
Zhong Wang (zhongwangchn@whu.edu.cn)
Renmin Hospital of Wuhan University: Wuhan University Renmin Hospital https://orcid.org/0000-0001-7072-2410

Research

Keywords: Breast cancer, PSMD8, KIF10, EMT, ERK pathway

Posted Date: September 14th, 2021

DOI: https://doi.org/10.21203/rs.3.rs-859898/v1

Abstract

Background

Breast cancer (BC) patients were threatened by distant metastasis and drug resistance for a long time. The mechanism was to be explored urgently. Proteasome 26S subunit non-ATPase 8 (PSMD8) was associated with protein degradation, but little was known about its role in BC.

Methods

The bioinformatics analysis was obtained from public databases. Breast cancer cell lines were knocked down or overexpressed PSMD8/kinesin family member 10 (KIF10) and detected their ability of proliferation and invasion. epithelial-to-mesenchymal transition (EMT)-related markers were detected by the western blot and immunohistochemistry. In vivo models were established to verify the effect of PSMD8 on tumor growth and distant metastasis. Cells were exposed to paclitaxel (PTX) and examined their apoptosis by flow cytometry.

Results

In the present study, we defined PSMD8 as a tumor-promoting molecule. PSMD8 was abnormally upregulated in BC tissues compared with adjacent tissues. High PSMD8 expression was related to poor prognosis in BC patients. The knockdown of PSMD8 attenuated the biological effect and epithelial-mesenchymal transition (EMT) progression in vitro and in vivo, and the overexpression of PSMD8 increased tumor progression in vitro. Furthermore, PSMD8 knockdown dramatically augmented the sensitivity of BC cells to paclitaxel, whereas PSMD8 overexpression showed the opposite effects. Mechanistic analysis indicated that PSMD8 activated the expression of kinesin family member 10 (KIF10) and its downstream extracellular regulated MAP kinase (ERK) signaling. Similar to PSMD8, we revealed that the expression of KIF10, which showed a positive correlation with PSMD8, was increased in BC tissues compared with adjacent tissues and associated with a poor prognosis of BC patients. The KIF10 knockdown significantly antagonized the facilitating effect of PSMD8 on the EMT program and chemotherapy tolerance. Finally, knocking down the level of KIF10 or inhibiting the ERK pathway in PSMD8-overexpressing cell lines partially blocked EMT progression and resistance against paclitaxel (PTX).

Conclusions

In conclusion, our results demonstrated that the PSMD8/KIF10 axis promoted BC development and PTX resistance via the ERK pathway. Our findings provide a theoretical basis for targeting PSMD8 to BC cells as a novel target for the treatment of BC.

Background

Breast cancer (BC) is the most common malignant carcinoma and the leading cause of cancer death among women[1]. The increased occurrence rate of metastasis exacerbates the mortality rate in BC. The 5-year overall survival rate without metastasis is over 80%, while distant metastasis reduces this rate to 25%[2,3]. Moreover, therapeutic resistance further hinders survival improvement. Hence, searching for new therapeutic targets is necessary.

The 26S proteasome is an adenosine triphosphate (ATP)-dependent protease associated with protein degradation and conjugated with multiple ubiquitins[4]. Proteasome 26S subunit, non-ATPase 8 (PSMD8, also known as RPN 12), is one of the components of the 19S regulator of the 26S proteasome[5]. The free PSMD8 subunit binding to the other eight subunits assembles the lid subcomplex of the 19S regulatory particle[6]. The latest research revealed that depletion of PSMD8 promoted epidermal aging[7]. In addition, a PSMD8 mutation was found in diffuse large B-cell lymphoma[8]. More importantly, the dysfunction of PSMD8 binding protein was related to tumor growth, invasion, and poor prognosis[9,10].Our previous study, revealed the tumor-promoting effect of PSMD12, another member of the proteasome subunit, in glioma[11]. Therefore, we inferred that PSMD8 has similar functions in BC.

The kinesin superfamily (KIFs) was characterized by microtubule-based motors. They function as intracellular transporters along microtubules in an ATP-dependent manner[12]. Forty-five KIFs have been discovered and illustrated to have different tumor pathobiologies[13]. KIF10 is localized on unattached kinetochores during mitosis and slides chromosomes to the spindle equator[14]. In the latest studies, KIF10 was reported to favor tumor initiation, development, and progression[15]. KIF10 was found to be upregulated in BC and hepatocellular carcinoma and was correlated with worse prognosis[15,16]. In estrogen receptor (ER)-positive BC, estrogen strongly induces KIF10 expression[17].

In this study, we demonstrated that PSMD8 served as a tumor-promoting factor. First, it was correlated with poor prognosis in BC. Second, PSMD8 stimulated BC progression and epithelial-to-mesenchymal transition (EMT) in vitro and in vivo. Moreover, we also provided evidence of the effect on attenuating paclitaxel sensitivity. Mechanistically, these effects were partially dependent on KIF10. Taken together, we explored the mechanism of PSMD8 in BC development and chemosensitivity.

Materials And Methods

Data acquisition

The expression of PSMD8 and KIF10 and their relationship with BC prognosis were analyzed by the UALCAN (http://ualcan.path.uab.edu) and GEPIA (http://gepia.cancer-pku.cn/) databases and Kaplan–Meier Plotter (https://kmplot.com/). Their mRNA profiling data were obtained from The Cancer Genome Atlas (TCGA) data portal (https://tcga-data.nci.nih.gov/tcga/) and GEO database.

Cell culture and reagents

Human breast cancer cell lines MDA-MB-231 and MCF7 were obtained from the American Type Culture Collection. Cells were cultured with the Dulbecco's modified Eagle's medium (DMEM, Gibco) containing 10% fetal bovine serum (FBS) and 1% penicillin-streptomycin at 37 °C. The U0126 (HY-12031) was purchased from MedChemExpress and dissolved in DMSO.

siRNAs and plasmid transfection

PSMD8 siRNA (5'- GCAGGGCACGAGTTATTTAAA), KIF10 siRNA (5'- GCUACUAAAUCAGGAGAAUTT), and scramble siRNA (5'-UUCUCCGAACGUGUCACGUTT-3') were purchased from GenPharma. Flag-PSMD8 and Flag-NC were purchased from GeneChem Co. Lipofectamine 2000 (Invitrogen, USA), and reduced serum medium (Opti-MEM, Gibco) were used according to the instructions. Human PSMD8 shRNA and control shRNA lentivirus were obtained from GeneChem Co.

Immunohistochemistry (IHC)

IHC was performed to examine the expression of PSMD8, KIF10, E-cadherin, snail, and Ki67. The scoring methods were described in a previous study[18]. All samples were categorized as negative, low expression or high expression according to the score.

Immunofluorescence (IF)

Treated cells were fixed with 4% paraformaldehyde at room temperature and perforated with 0.2% Triton-X 100 for 15 min at 4 °C. BSA (2%) was prepared for blocking for 1 h at room temperature. The primary antibody was prepared with 1% BSA. Cells were incubated with the corresponding primary antibody overnight at 4 °C and then 488-conjugated (Invitrogen, A-11034), and 568-conjugated (Invitrogen, A-11011) antibodies for 30 min at room temperature. All samples were stained with DAPI for 3 min. Fluorescence images were obtained by fluorescence microscopy.

Western blot (WB)

The procedure of WB was described as previous[11]. The membrane was blocked in 5% fat-free milk for 2 h at room temperature and incubated with primary antibody overnight at 4 °C. Finally, the membranes were incubated with secondary antibodies for 1 h at room temperature. All antibodies are listed in Supplementary Table 1.

Cell Counting Kit-8 assay (CCK8)

Two thousand treated cells were seeded on the 96-well plate. Ten microliters of CCK8 (CK04, Dojindo, Japan) solution was added to each well. After 2 h incubation, the absorbance was determined at 450 nm.

Transwell assay

Treated cells were seeded in the upper chambers with Matrigel in serum-free medium, and DMEM with 10% FBS was added to the lower chamber. Cells were cultured for 24 h, fixed, and stained with 0.1%

crystal violet.

Flow cytometry (FCM)

After a series of treatments, cells were washed with PBS and digested with non-EDTA trypsin enzyme. Cells were suspended in a culture medium and centrifuged at 1000 rpm for 5 minutes. Discarding the supernatant and resuspending in PBS, we centrifuged at 1000 rpm for 5 minutes again. Double staining with Annexin V-FITC and propidium iodide (PI) (Biouniquer, BU-AP0103) was performed and incubated for 15 min. The results were determined by FCMcan flow cytometry (FASC Calibur, BD, USA).

Animal experiments

MDA-MB-231 cells were infected with LV-shPSMD8 and LV-shCtrl lentiviruses (GeneChem Co., Shanghai, China). A total of 2.5×10^6 cells per mouse were inoculated into the right iliac fossa of 4-week-old female BALB/c nude mice. After 6 weeks of feeding, the mice were sacrificed, and the xenografts were separated for further analysis.

Similarly, LV-shPSMD8 and LV-shCtrl cells were also injected into the fourth mammary fat pad (1×10^6 cells per mouse). When the tumor size reached $^{\text{approximately 300 mm3}}$, tumors were removed, and the mice were sacrificed 10 days after the operation. The lung tissues were separated and fixed. Hematoxylin and eosin (HE) staining was performed to demonstrate lung metastasis.

Statistical analysis

Data were analyzed by one-way ANOVA with SPSS 22.0. The graphs were made by GraphPad Prism 6. Independent experiments were repeated at least three times. $P<0.05$ indicated statistically significant.

Results

High PSMD8 expression was correlated with poor survival in BC patients

We analyzed the expression of PSMD8 in nontumor breast tissue and tumor tissue from GEPIA and UALCAN. The level of PSMD8 expression was significantly upregulated in tumor tissue compared with normal tissue (**Fig. 1A-B**). Similarly, IHC staining demonstrated the same result (**Fig. 1D**). Moreover, the PSMD8 transcripts were positively correlated with tumor stage and lymphatic metastasis stage (**Fig. 1C, E-F**). Kaplan–Meier (K-M) analysis of recurrence-free survival (RFS), and overall survival (OS) showed that high expression of PSMD8 was associated with poor survival (**Fig. 1G-H**). In particular, a high level of PSMD8 implied worse RFS in lymphatic metastatic BC patients (**Fig. 1I**). Taken together, the bioinformatics analysis and IHC staining reminded us that PSMD8 was upregulated in tumor tissue and was associated with poor prognosis in BC.

PSMD8 promoted cell growth and invasion in vitro

To explore the effect of PSMD8 on the biological behavior of MDA-MB-231 and MCF7 breast cancer cell lines, we used PSMD8 siRNA and plasmids to downregulate and upregulate the expression level of PSMD8 in cells, respectively. We first displayed the efficiency of PSMD8 knockdown (KD) and overexpression (OE) (**Fig. 2A and D**). A CCK-8 assay was performed to test tumor proliferation after the corresponding treatments. PSMD8 knockdown attenuated tumor growth, while PSMD8 overexpression enhanced tumor growth (**Fig. 2B and E**). In addition, cell invasion was also decreased as PSMD8 was knocked down and increased as PSMD8 was overexpressed (**Fig. 2C and F**). In brief, PSMD8 promoted proliferation and invasion in BC cells.

PSMD8 triggered EMT program in BC cells

Given the correlation between EMT and tumor development, we further explored the role of PSMD8 in EMT progression. We knocked down the expression of PSMD8 and detected the protein levels of the EMT-related proteins E-cadherin (E-cad) and Snail. The WB results showed that the level of E-cad was upregulated, and snail was downregulated in $PSMD8^{KD}$ cells. The opposite results were observed in $PSMD8^{OE}$ cells (**Fig. 3A-B**). In parallel, the picture of IF confirmed this phenomenon as well. The level of E-cad was strengthened, and the level of snail was weakened in $PSMD8^{KD}$ cells (**Fig. 3C**). In addition, IHC was performed to detect the levels of PSMD8 and E-cad in BC tissues. The tissue with a high expression level of PSMD8 showed a low expression level of E-cad, and the tissue with low expression of PSMD8 displayed a high expression level of E-cad (**Fig. 3D**). Furthermore, we overexpressed PSMD8 in $PSMD8^{KD}$ cells and detected the protein levels of E-cad and snail. The WB results illustrated that PSMD8 overexpression reversed the effect of PSMD8 knockdown (**Fig. 3E**). In summary, PSMD8 promoted EMT progression in vitro.

Inhibition of PSMD8 suppressed tumor growth and lung metastasis in vivo

We established xenograft models to verify the effect of PSMD8 in vivo. First, LV-shPSMD8 was applied to MDA-MB-231 cells to establish stably silenced cells (**Fig. 4A-B**). A photograph of xenografts is displayed (**Fig. 4C**), and their weights were compared. The mean weight of the shPSMD8 group was significantly less than that of its counterpart (**Fig. 4D**).

Additionally, we infected mice with the treated cells in situ and detected lung metastasis. The separated lung tissue showed that the number of lung metastatic nodules was lower in the shPSMD8 group (**Fig. 4E**). HE staining demonstrated the same trend (**Fig. 4F**). In addition, we detected the levels of Ki67 and E-cad in tumors removed from xenograft models. IHC staining showed that E-cad expression increased, while the expression of Ki67 decreased after PSMD8 was silenced (**Fig. 4G**). In summary, this phenomenon suggested that silencing PSMD8 impaired the growth of breast tumors and decreased lung metastasis.

PSMD8 mediated the expression of KIF10

According to the TCGA and GSE1456 databases, the expression of PSMD8 was positively correlated with the expression of KIF10 (**Fig. 5A-B**). Furthermore, the WB results showed that the protein level of KIF10 was decreased after PSMD8 knockdown and increased after PSMD8 overexpression (**Fig. 5C**). Parallel effects were observed in BC patient tissues by IHC staining (**Fig. 5D**). Additionally, the protein levels of PSMD8 and KIF10 in xenografts were detected by IHC, which illustrated that the level of KIF10 declined in the shPSMD8 group compared with the shCtrl group (**Fig. 5E**). More important, K-M analysis showed that the prognosis of BC patients with high levels of PSMD8 and KIF10 was worse than the prognosis of BC patients with low levels of both PSMD8 and KIF10 in GES1456 database (**Fig. 5F**). Overall, the expression of KIF10 was regulated by PSMD8 and was positively correlated.

High KIF10 expression was correlated with poor survival in BC patients

Analysis from GEPIA, UALCAN and IHC staining demonstrated that the expression of KIF10 was higher in tumor tissue than in normal tissue (**Fig. 6A-B and D**), regardless of the subtype of BC (**Fig. 6C**). Moreover, the levels of KIF10 transcripts were positively associated with the BC stage and lymphatic metastasis stage (**Fig. 6E-F**). The K-M analysis of OS and RFS in all patients showed that the higher the expression of KIF10, the worse the prognosis was, particularly the RFS in lymphatic metastatic patients (**Fig. 6G-I**). In short, tumor tissue had higher KIF10 expression than normal tissue and was correlated with a poor prognosis.

KIF10 knockdown decreased cell growth and invasion in vitro

We will explore the exact effect of KIF10 on the biological functions of BC cells. The knockdown efficiency of KIF10 in BC cells is shown in **Fig. 7A**. CCK-8 and Transwell assays were performed to detect the proliferation and invasion abilities of BC cell lines. The results demonstrated that cell proliferation ability and the ratio of cell invasion were decreased after KIF10 knockdown (**Fig. 7B-C**). In addition, similar to PSMD8, the WB results showed that the expression level of E-cad was increased and the level of Snail was decreased in KIF10-knockdown cells (**Fig. 7D**). Furthermore, the expression of PSMD8 was positively correlated with the expression of KIF10 (**Fig. 7E**). These results suggested that KIF10 was capable of impairing tumor progression.

PSMD8/KIF10 axis promoted tumor development in vitro

Given that both PSMD8 and KIF10 promoted tumor development and that these two had a positive correlation, we further verified their link and effect. FCM were performed to detect apoptosis in $PSMD8^{KD}$ cells and $KIF10^{KD}$ cells under paclitaxel (PTX) conditions. Knockdown of either PSMD8 or KIF10 significantly enhanced PTX-induced the rate of cell apoptosis (**Fig 8A-B**), while the two proteins overexpression significantly antagonized PTX-induced apoptosis in BC cells (**Fig 8C-D**). Furthermore, knocking down the expression of KIF10 in $PSMD8^{OE}$ cells partially reversed the protective effect of PSMD8 against PTX (**Fig 8C-D**). Similarly, cell proliferation and invasion also decreased (**Fig 8E-F**). EMT-related markers were detected by the WB. Rescue experiments illustrated that

the expression of E-cad increased and snail decreased (**Fig 8G**). In summary, the PSMD8-KIF10 axis could decrease chemosensitivity to PTX and enhance EMT progression.

Extracellular signal-regulated kinase 1/2 (ERK) signaling is essential for EMT and chemosensitivity mediated by the PSMD8/KIF10 axis in BC

To further explore the involved signaling pathways, the protein levels of p-ERK and ERK were detected. The ratio of p-ERK/ERK significantly decreased in both $PSMD8^{KD}$ and $KIF10^{KD}$ cells (**Fig. 9A**), while PSMD8 overexpression significantly enhanced the activation of ERK pathway (**Fig. 9B**). In addition, the ratio of p-ERK/ERK returned after the knockdown of KIF10 in $PSMD8^{OE}$ cells (**Fig. 9B**). Furthermore, the inhibitor of ERK signaling, U0126, was used to treat $PSMD8^{OE}$ cells. FMC demonstrated that overexpression of PSMD8 significantly protected tumor cells from PTX, but U0126 partially blocked this effect (**Fig. 9C-D**). Meanwhile, it also attenuated the cell proliferation and invasion effects of PSMD8 (**Fig. 9E-F**). Furthermore, the protein level of E-cad was increased, and the level of snail was decreased after U0126 treatment in $PSMD8^{OE}$ cells (**Fig. 9G**). In short, the ERK signaling pathway was involved in tumor proliferation and invasion regulated by the PSMD8/KIF10 axis. Inhibition of the ERK pathway could retard PSMD8/KIF10-induced EMT and enhance sensitivity to PTX.

Discussion

Due to aggressive BC threats, searching for new therapeutic targets is urgent. In this study, we found that PSMD8 was highly expressed in tumor tissue and was negatively associated with the survival of BC patients. Experiments performed in vitro verified that PSMD8 could promote tumor growth and invasion, which was also confirmed in vivo. Mechanistically, KIF10 could modulate EMT progression in response to the expression of PSMD8. The application of an ERK inhibitor impaired tumor growth and invasion induced by the PSMD8/KIF10 axis and attenuated the protective effect of PSMD8 from PTX.

The 26S proteasome is the endpoint for the ubiquitin-proteasome system, whose function ranges from protein homeostasis to cellular processes such as signal transduction and stress responses[19]. PSMD8 was reported to be overexpressed in breast cancer tissues[20], consistent with our results. However, almost no study has demonstrated the effect and mechanism of PSMD8 in tumor development. As a structural component of the proteasome, PSMD8 should have a similar function to other subunits. PSMD14 promotes tumor growth and metastasis in gliomas[21,] hepatocellular carcinoma,[22] and esophageal squamous cell carcinoma[23]. Its contributions to tumorigenesis and chemoresistance were also observed in colorectal cancers[24]. Obviously, cell growth and invasion were enhanced after PSMD8 overexpression, as well in our report. The results of FCM verified the increased sensitivity to PTX after knocking down the expression of PSMD8. In addition, mass spectrometry to examine the interaction between snail and deubiquitinases illustrated that PSMD14 targeted snail for deubiquitination and stabilization, thus mediating snail-induced EMT[23]. In this study, we detected the expression of snails after PSMD8 interference and overexpression. PSMD8 favored the expression of snail and EMT progression.

The kinesin family is essential for mitosis and chromosome alignment[14]. It was likely that KIF10 was related to cell proliferation. Thus, we provided evidence that KIF10 was involved in cell growth in vitro and in vivo. KIF10 was overexpressed in BC and hepatocellular carcinoma and was associated with worse OS, RFS, and distant metastasis-free survival[15,16]. However, only bioinformatics analysis was provided to support their perspectives. The results of our study further verified their hypothesis. IHC staining and WB illustrated that KIF10 was highly expressed in tumor tissues and was regulated by PSMD8. Moreover, knocking down KIF10 can significantly reduce the proliferation rate, invasion ability, and EMT process of BC cells. Furthermore, PSMD8 promoted snail-induced EMT through KIF10 activation. The application of an ERK inhibitor suggested that KIF10 modulated EMT progression via the ERK pathway. A study revealed that KIF10 was stimulated by ER, which gave rise to tumor growth. Moreover, KIF10, but of the same family, was illustrated to be crucial for the survival of tamoxifen-sensitive and tamoxifen-resistant BC cells[17]. It was also supported our study that KIF10 contributed to PTX resistance.

ERK is localized in the cytoplasm of resting cells, an evolutionarily conserved signaling pathway that transmits information from the cell surface to promote cell proliferation and survival. Dysregulation of the ERK pathway is involved in the induction of primary cancer[25]. Hyperexpression of ERK activated the antiapoptotic molecule BCL2 in BC, resulting in drug resistance[26], consistent with our research showing that inhibition of the ERK pathway led to increased apoptosis in $PSMD8^{OE}$ cells treated with PTX. In addition, ERK signaling was reported to control the G1/S phase of the cell cycle in proliferating cells[27]. The activation of ERK induced the response to mitogens[28], which suggested its link with KIF10 and proliferative effect.

Conclusions

In conclusion, we identified PSMD8 as a tumor promoter and initially explored its mechanism. The PSMD8/KIF10 axis mediated the activation of the ERK pathway, consequently favoring tumor progression and chemotherapy resistance. The results of this research clarify that the PSMD8/KIF10 axis plays a vital role in the progression of BC and provide novel potential therapeutic targets for the precise treatment of BC.

Declarations

Ethics approval and consent to participate

Breast cancer tissues and normal breast tissues were collected at Renmin Hospital of Wuhan University. All procedures performed in this study was carried out according to the principles of the Ethics Committee of Renmin Hospital of Wuhan University. The animal experiment complied with the principles of the Animal Centre of the Renmin Hospital of Wuhan University.

Consent for publication

All the listed authors have approved the submitted manuscript.

Availability of data and materials

All the data and material could be traced from the paper or can be requested from the public databases.

Competing interests

The authors declare that they have no competing interests.

Funding

This work was partially supported by a National Natural Science Foundation of China (NSFC) grant (grant No.: 81471781) and a National Major Scientific Instruments and Equipment Development Projects grant (grant No.: 2012YQ160203) to Prof. Shengrong Sun, the Natural Science Foundation of Hubei Province (2020CFA026) by Prof. Yi Tu.

Authors' contributions

LZ, LS and WZ contributed to the experiment design; LZ and LC contributed to the acquisition of data; WZ, LZ, LC, TY, YF and SS contributed to the analysis, and interpretation of data; WZ contributed to the study supervision; LZ and LC contributed to the drafting of manuscript; LS and WZ contributed to the revision of manuscript. All authors have read and approved the final manuscript.

Acknowledgements

We would like to thank the participating patients for the source of BC tissue specimens.

References

1. Britt KL, Cuzick J, Phillips KA. Key steps for effective breast cancer prevention. *Nat Rev Cancer.* 2020;20(8):417-436.
2. Allemani C, Matsuda T, Di Carlo V, et al. Global surveillance of trends in cancer survival 2000-14 (CONCORD-3): analysis of individual records for 37 513 025 patients diagnosed with one of 18 cancers from 322 population-based registries in 71 countries. *Lancet.* 2018;391(10125):1023-1075.
3. Liang Y, Zhang H, Song X, Yang Q. Metastatic heterogeneity of breast cancer: Molecular mechanism and potential therapeutic targets. *Semin Cancer Biol.* 2020;60:14-27.
4. Smalle J, Kurepa J, Yang P, et al. Cytokinin growth responses in Arabidopsis involve the 26S proteasome subunit RPN12. *Plant Cell.* 2002;14(1):17-32.
5. Yi YJ, Manandhar G, Sutovsky M, Jonakova V, Park CS, Sutovsky P. Inhibition of 19S proteasomal regulatory complex subunit PSMD8 increases polyspermy during porcine fertilization in vitro. *J Reprod Immunol.* 2010;84(2):154-163.

6. Tomko RJ, Jr., Hochstrasser M. Incorporation of the Rpn12 subunit couples completion of proteasome regulatory particle lid assembly to lid-base joining. *Mol Cell.* 2011;44(6):907-917.
7. Ishii MA, Miyachi KJ, Cheng B, Sun BK. Aging-Associated Decline of Epidermal PSMD8 Contributes to Impaired Skin Function. *J Invest Dermatol.* 2018;138(4):976-978.
8. Zhang S, Wang L, Cheng L. Aberrant ERG expression associates with downregulation of miR-4638-5p and selected genomic alterations in a subset of diffuse large B-cell lymphoma. *Mol Carcinog.* 2019;58(10):1846-1854.
9. Ke W, Lu Z, Zhao X. NOB1: A Potential Biomarker or Target in Cancer. *Curr Drug Targets.* 2019;20(10):1081-1089.
10. Dong S, Xue S, Sun Y, et al. MicroRNA-363-3p downregulation in papillary thyroid cancer inhibits tumor progression by targeting NOB1. *J Investig Med.* 2021;69(1):66-74.
11. Wang Z, Li Z, Xu H, et al. PSMD12 promotes glioma progression by upregulating the expression of Nrf2. *Ann Transl Med.* 2021;9(8):700.
12. Hirokawa N, Noda Y, Tanaka Y, Niwa S. Kinesin superfamily motor proteins and intracellular transport. *Nat Rev Mol Cell Biol.* 2009;10(10):682-696.
13. Miki H, Setou M, Kaneshiro K, Hirokawa N. All kinesin superfamily protein, KIF, genes in mouse and human. *Proc Natl Acad Sci U S A.* 2001;98(13):7004-7011.
14. Craske B, Welburn JPI. Leaving no-one behind: how CENP-E facilitates chromosome alignment. *Essays Biochem.* 2020;64(2):313-324.
15. Li TF, Zeng HJ, Shan Z, et al. Overexpression of kinesin superfamily members as prognostic biomarkers of breast cancer. *Cancer Cell Int.* 2020;20:123.
16. Li X, Huang W, Huang W, et al. Kinesin family members KIF2C/4A/10/11/14/18B/20A/23 predict poor prognosis and promote cell proliferation in hepatocellular carcinoma. *Am J Transl Res.* 2020;12(5):1614-1639.
17. Zou JX, Duan Z, Wang J, et al. Kinesin family deregulation coordinated by bromodomain protein ANCCA and histone methyltransferase MLL for breast cancer cell growth, survival, and tamoxifen resistance. *Mol Cancer Res.* 2014;12(4):539-549.
18. Wang Z, Li Z, Wu Q, et al. DNER promotes epithelial-mesenchymal transition and prevents chemosensitivity through the Wnt/beta-catenin pathway in breast cancer. *Cell Death Dis.* 2020;11(8):642.
19. Bard JAM, Goodall EA, Greene ER, Jonsson E, Dong KC, Martin A. Structure and Function of the 26S Proteasome. *Annu Rev Biochem.* 2018;87:697-724.
20. Deng S, Zhou H, Xiong R, et al. Over-expression of genes and proteins of ubiquitin specific peptidases (USPs) and proteasome subunits (PSs) in breast cancer tissue observed by the methods of RFDD-PCR and proteomics. *Breast Cancer Res Treat.* 2007;104(1):21-30.
21. Zhi T, Jiang K, Xu X, et al. ECT2/PSMD14/PTTG1 axis promotes the proliferation of glioma through stabilizing E2F1. *Neuro Oncol.* 2019;21(4):462-473.

22. Lv J, Zhang S, Wu H, et al. Deubiquitinase PSMD14 enhances hepatocellular carcinoma growth and metastasis by stabilizing GRB2. *Cancer Lett.* 2020;469:22-34.
23. Zhu R, Liu Y, Zhou H, et al. Deubiquitinating enzyme PSMD14 promotes tumor metastasis through stabilizing SNAIL in human esophageal squamous cell carcinoma. *Cancer Lett.* 2018;418:125-134.
24. Seo D, Jung SM, Park JS, et al. The deubiquitinating enzyme PSMD14 facilitates tumor growth and chemoresistance through stabilizing the ALK2 receptor in the initiation of BMP6 signaling pathway. *EBioMedicine.* 2019;49:55-71.
25. Maik-Rachline G, Hacohen-Lev-Ran A, Seger R. Nuclear ERK: Mechanism of Translocation, Substrates, and Role in Cancer. *Int J Mol Sci.* 2019;20(5).
26. Liu F, Yang X, Geng M, Huang M. Targeting ERK, an Achilles' Heel of the MAPK pathway, in cancer therapy. *Acta Pharm Sin B.* 2018;8(4):552-562.
27. Voisin L, Saba-El-Leil MK, Julien C, Fremin C, Meloche S. Genetic demonstration of a redundant role of extracellular signal-regulated kinase 1 (ERK1) and ERK2 mitogen-activated protein kinases in promoting fibroblast proliferation. *Mol Cell Biol.* 2010;30(12):2918-2932.
28. Fowler T, Sen R, Roy AL. Regulation of primary response genes. *Mol Cell.* 2011;44(3):348-360.

Figures

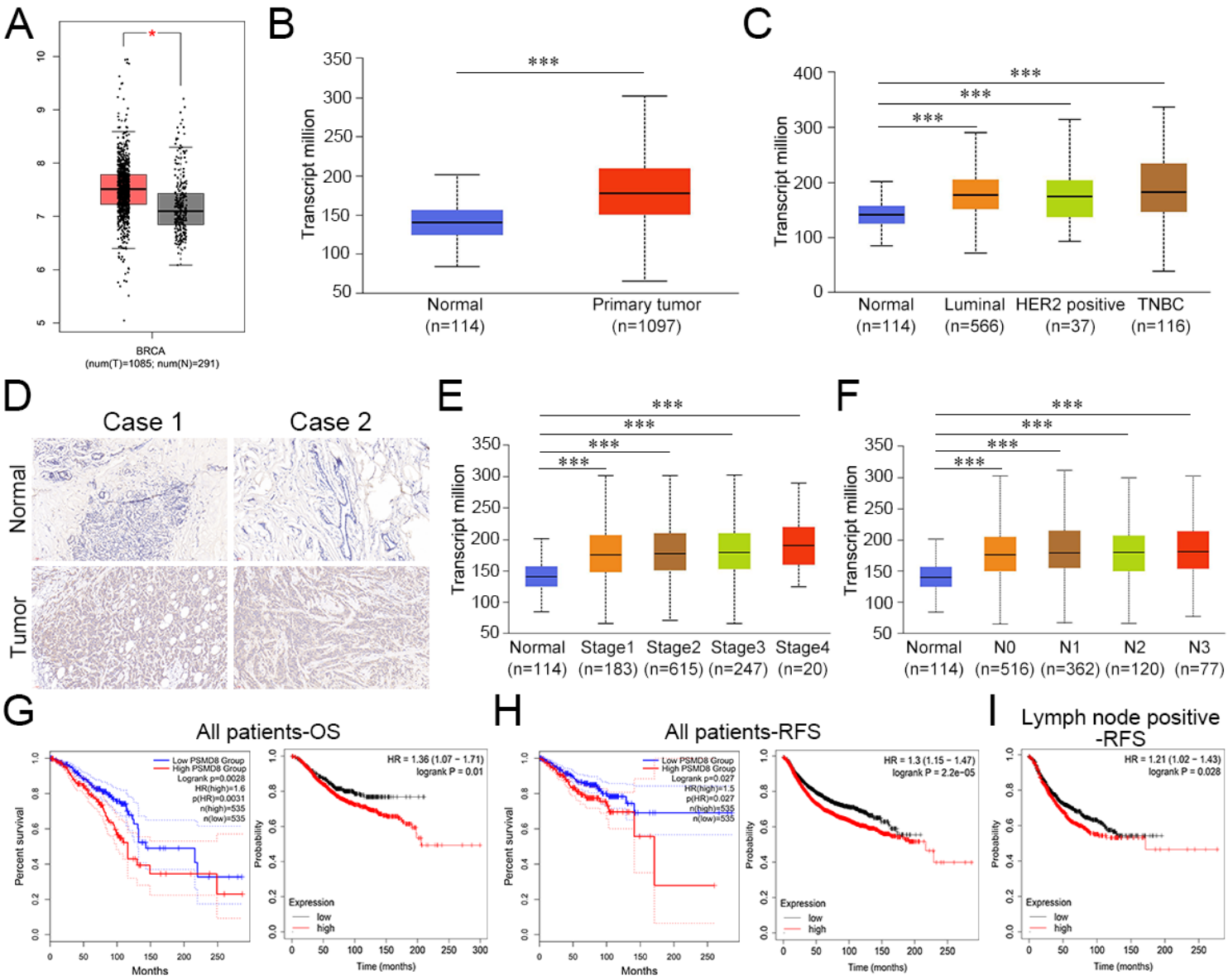

Figure 1

Elevated PSMD8 expression indicated poor survival in BC patients. (A-B) PSMD8 expression in BC tissues and adjacent tissues from GEPIA and UALCAN. (C) KIF10 expression in different types of BC from UALCAN. (D) IHC staining for PSMD8 in BC tissues and adjacent tissues. (E) PSMD8 expression in different stages of BC from UALCAN. (F) PSMD8 expression in different lymphatic metastasis stages of BC from UALCAN. (G) OS of BC patients from GEPIA and K-M Plotter. (H) RFS of BC patients from GEPIA and K-M Plotter. (I) RFS of lymphatic metastatic BC patients from K-M Plotter. *p < 0.05 and ***p < 0.001 compared with the control group.

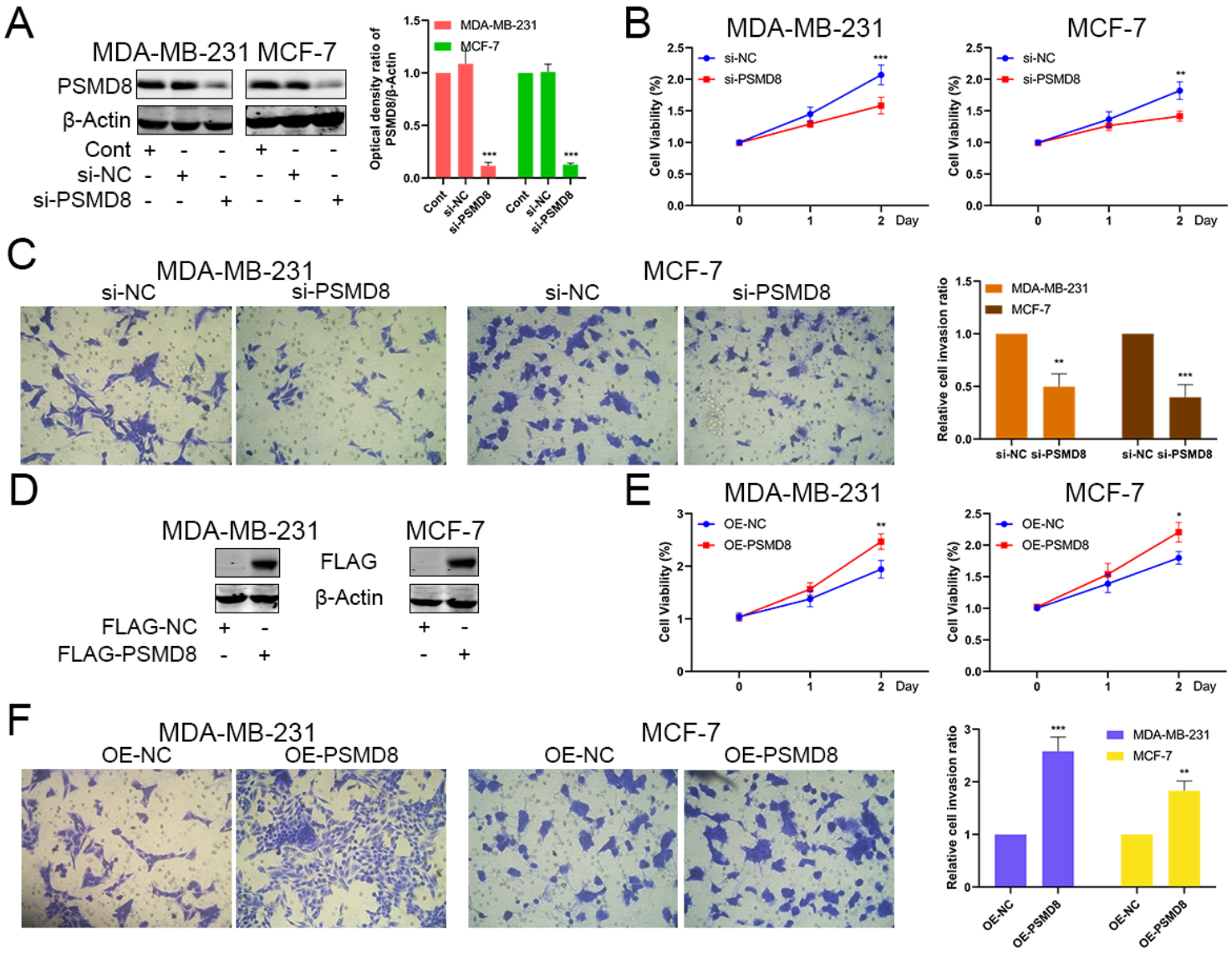

Figure 2

PSMD8 promoted cell proliferation and a prometastatic phenotype in BC cells. (A, D) Knockdown and overexpression efficiency of PSMD8 in MDA-MB-231 and MCF7 cell lines. (B, E) CCK-8 assay performed in knockdown and overexpressed cell lines. (C, F) Transwell assays performed in knockdown and overexpressed cell lines (magnification 200×). The values are presented as the means ± SD from three independent experiments. *p<0.05, **p<0.01, and ***p<0.001 compared with the control group.

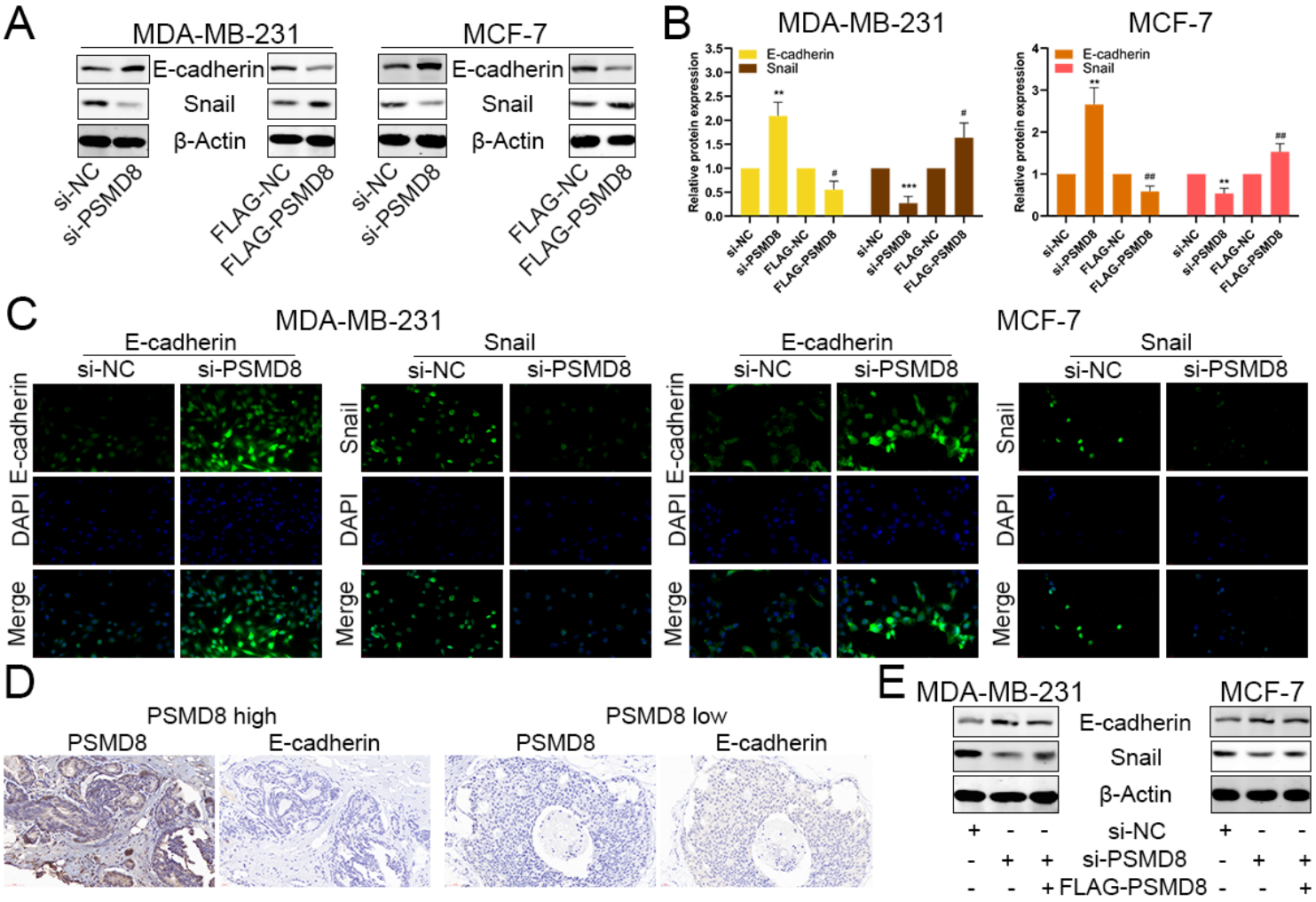

Figure 3

PSMD8 promoted the EMT progress. (A-B) EMT-related protein levels in PSMD8-knockdown and PSMD8-overexpression cell lines. (C) IF images of PSMD8 and EMT-related markers (E-cad and snail) in BC cell lines (magnification 630×). (D) IHC staining images of PSMD8 and E-cad in BC samples (magnification 200×). (E) PSMD8 was overexpressed in PSMD8KD cells. The WB analysis detected E-cad and Snail. The values are presented as the means ± SD from three independent experiments. #p<0.05, ##p<0.01, *p<0.05, **p<0.01, and ***p<0.001 compared with the control group.

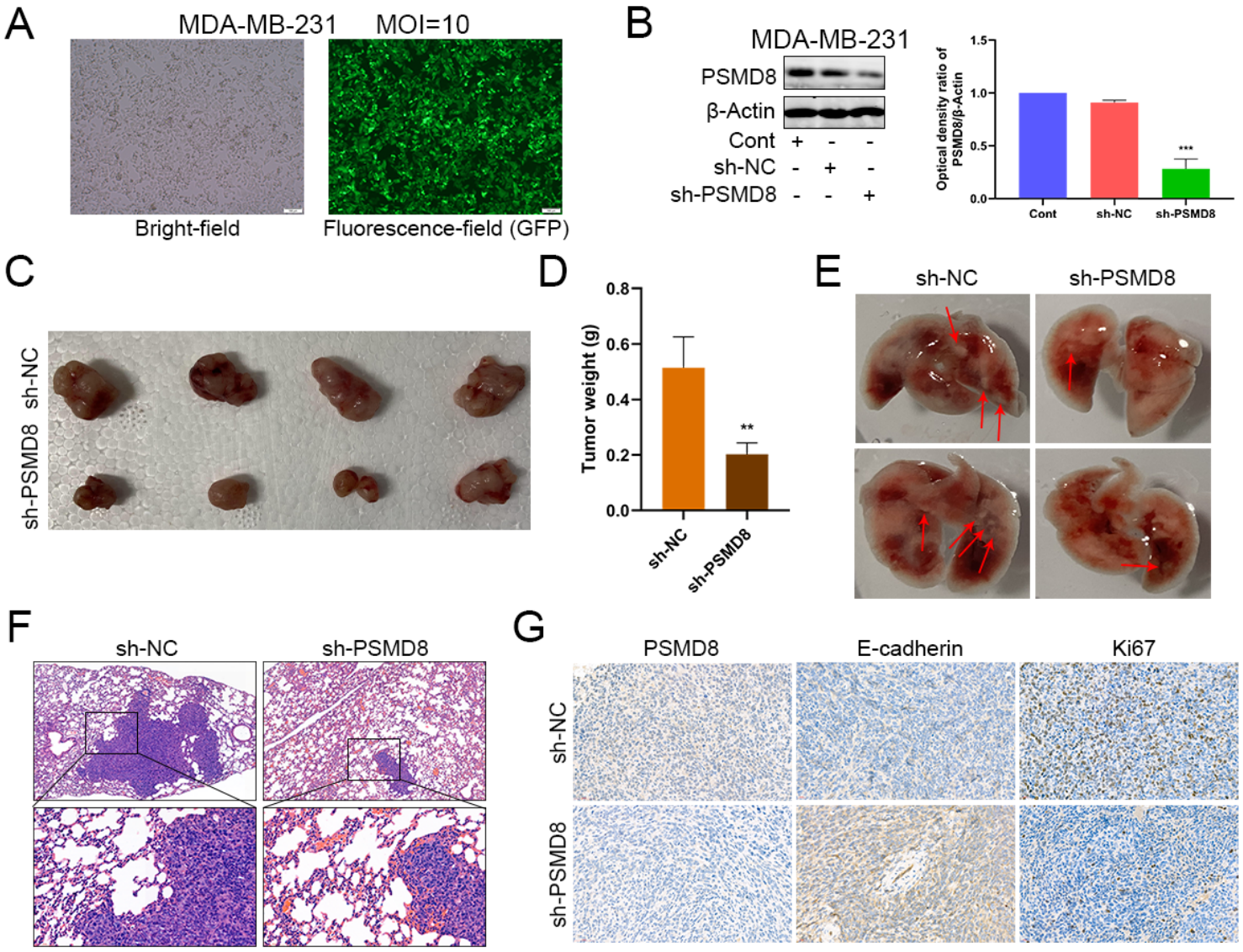

Figure 4

Inhibition of PSMD8 suppressed tumor growth and metastasis in vivo. (A) Infection efficiency of stable PSMD8 knockdown in MDA-MB-231 cells by fluorescence microscopy. (B) Infection efficiency of PSMD8 knockdown in MDA-MB-231 cells by WB. (C) Tumors dissected from various groups of mice. (D) Tumor weight from various groups of mice. (E) Bright field images of lung metastasis in the control group and knockdown group. (F) HE staining of metastatic lung tumors. (G) IHC staining of PSMD8, Ki67 and E-cad in xenografts from various groups. The values are presented as the means ± SD from three independent experiments. **p<0.01, and ***p<0.001 compared with the control group.

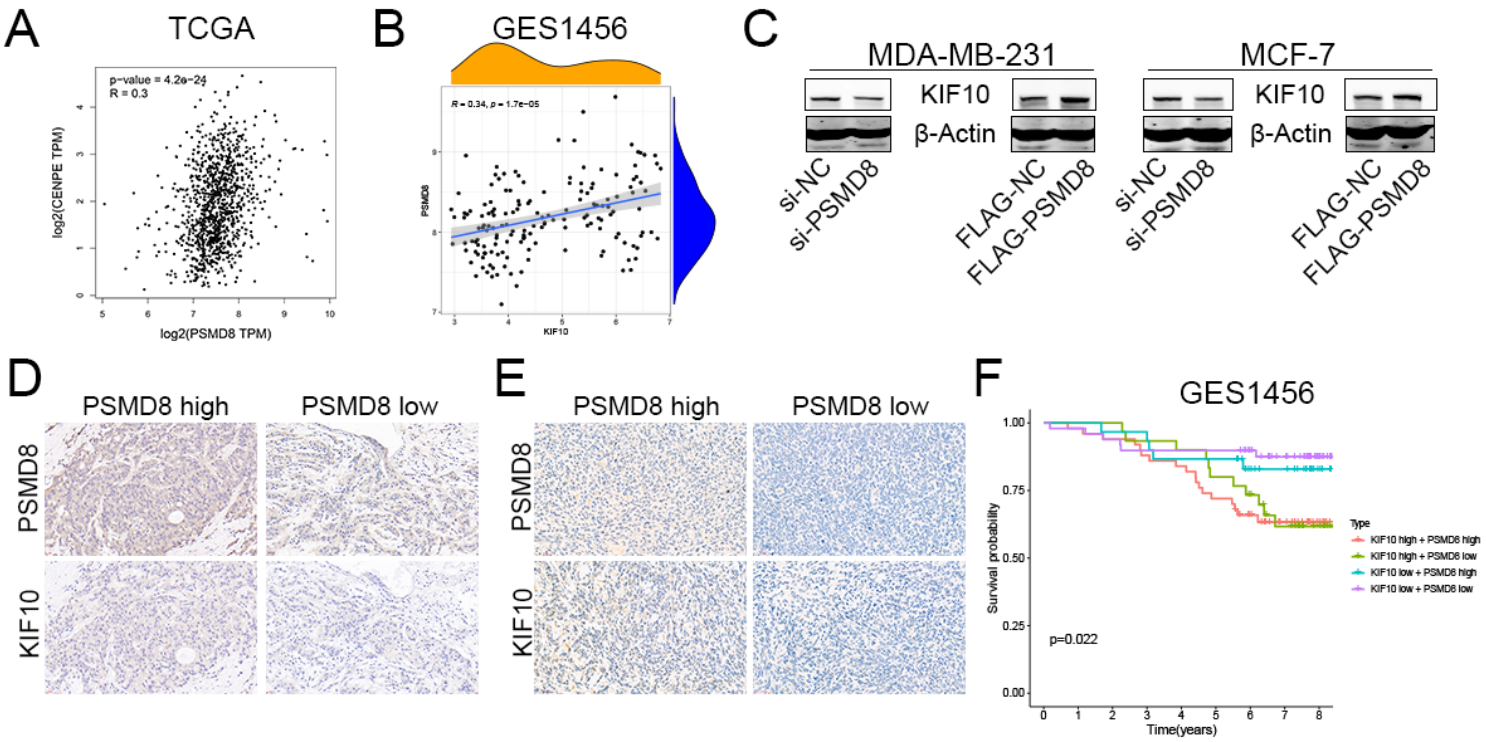

Figure 5

PSMD8 positively regulated the expression of KIF10. (A) The correlation between PSMD8 and KIF10 from GEPIA. (B) The correlation between PSMD8 and KIF10 from GES1456 database. (C) The expression of KIF10 was measured by WB in PSMD8-knockdown and PSMD8-overexpression cells. (D) IHC staining images of PSMD8 and KIF10 in BC samples (magnification 200×). (E) IHC staining of PSMD8 and KIF10 in xenografts. The values are presented as the means ± SD from three independent experiments.

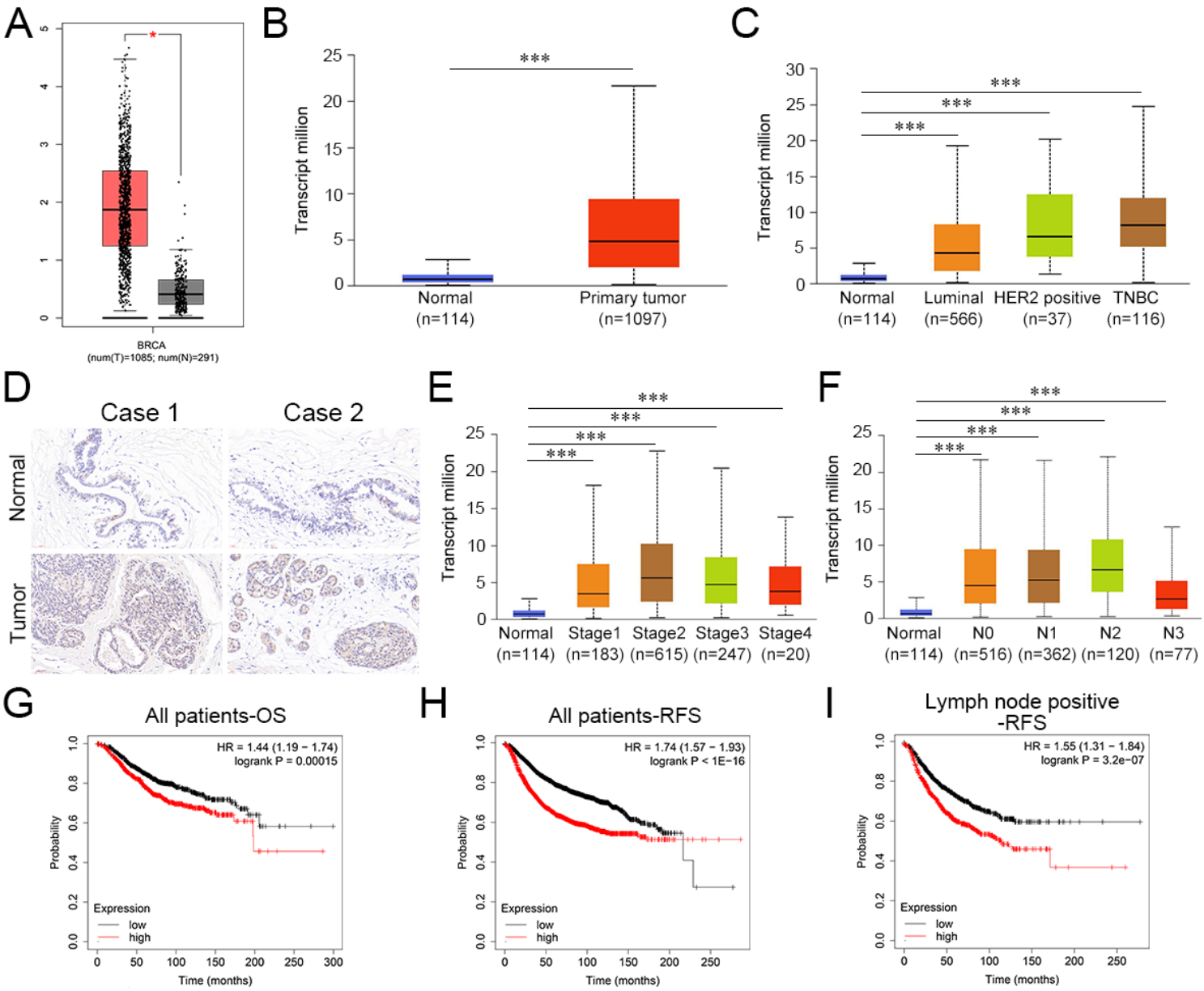

Figure 6

Elevated KIF10 expression indicated poor survival in BC patients. (A-B) KIF10 expression in BC tissues and adjacent tissues from GEPIA and UALCAN. (C) KIF10 expression in different types of BC from UALCAN. (D) IHC staining for KIF10 in BC tissues and adjacent tissues. (E) KIF10 expression in different stages of BC from UALCAN. (F) PSMD8 expression in different lymphatic metastasis stages of BC from UALCAN. (G) OS of BC patients from K-M Plotter. (H) RFS of BC patients from and K-M Plotter. (I) RFS of lymphatic metastatic BC patients from the K-M Plotter. The values are presented as the means ± SD from three independent experiments. *p<0.05 and ***p<0.001 compared with the corresponding group.

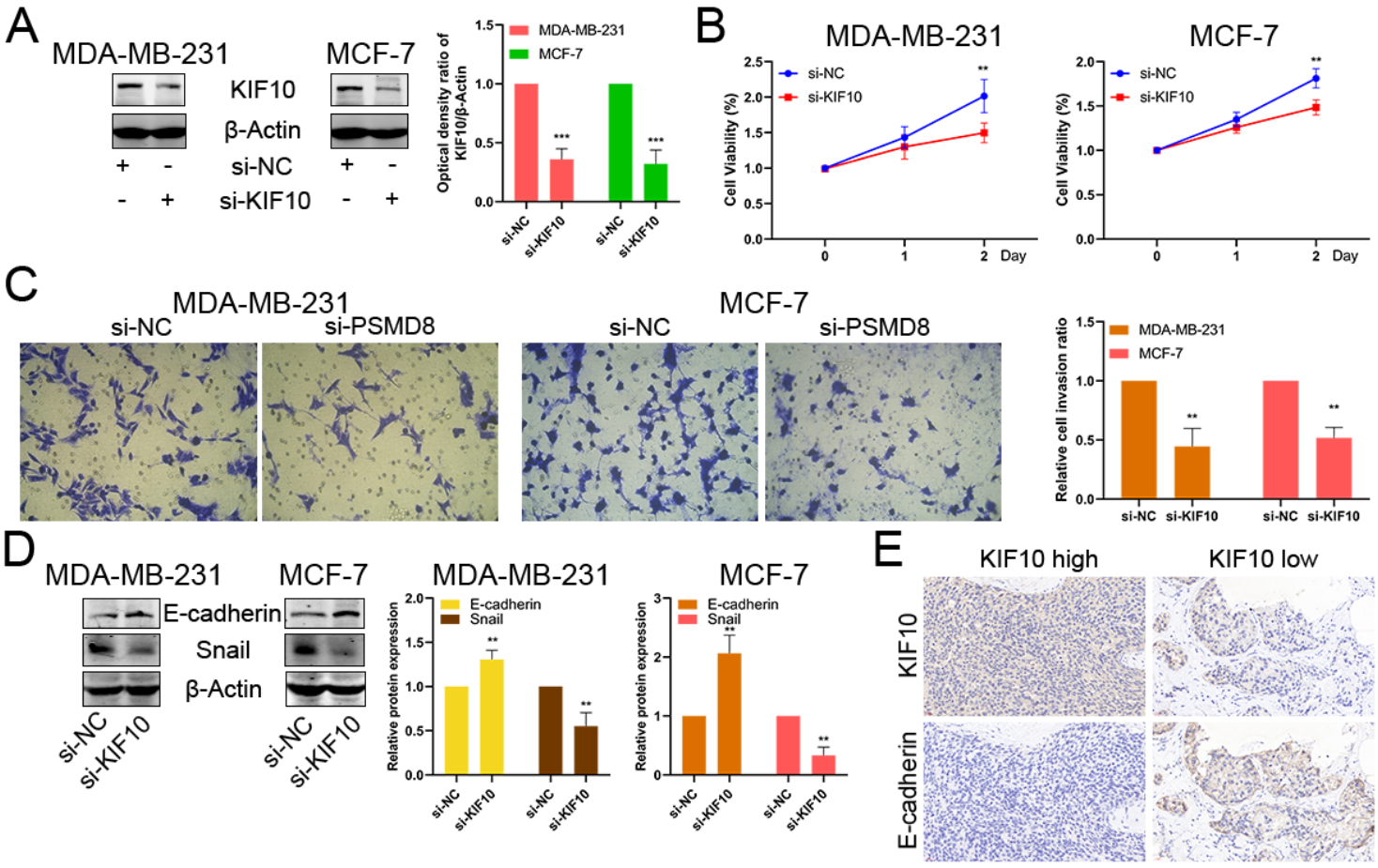

Figure 7

Knockdown of KIF10 attenuated cell proliferation and the prometastasis phenotype in BC cells. (A) Knockdown efficiency of KIF10 in MDA-MB-231 and MCF7 cell lines. (B) CCK-8 assay performed in KIF10 knockdown cell lines. (C) Transwell assay performed in KIF10 knockdown cell lines. (magnification 200×). D) IHC staining images of PSMD8 and E-cad in BC samples (magnification 200×). (E) EMT-related protein levels in KIF10-knockdown cell lines. The values are presented as the means ± SD from three independent experiments. **p<0.01 and ***p<0.001 compared with the corresponding group.

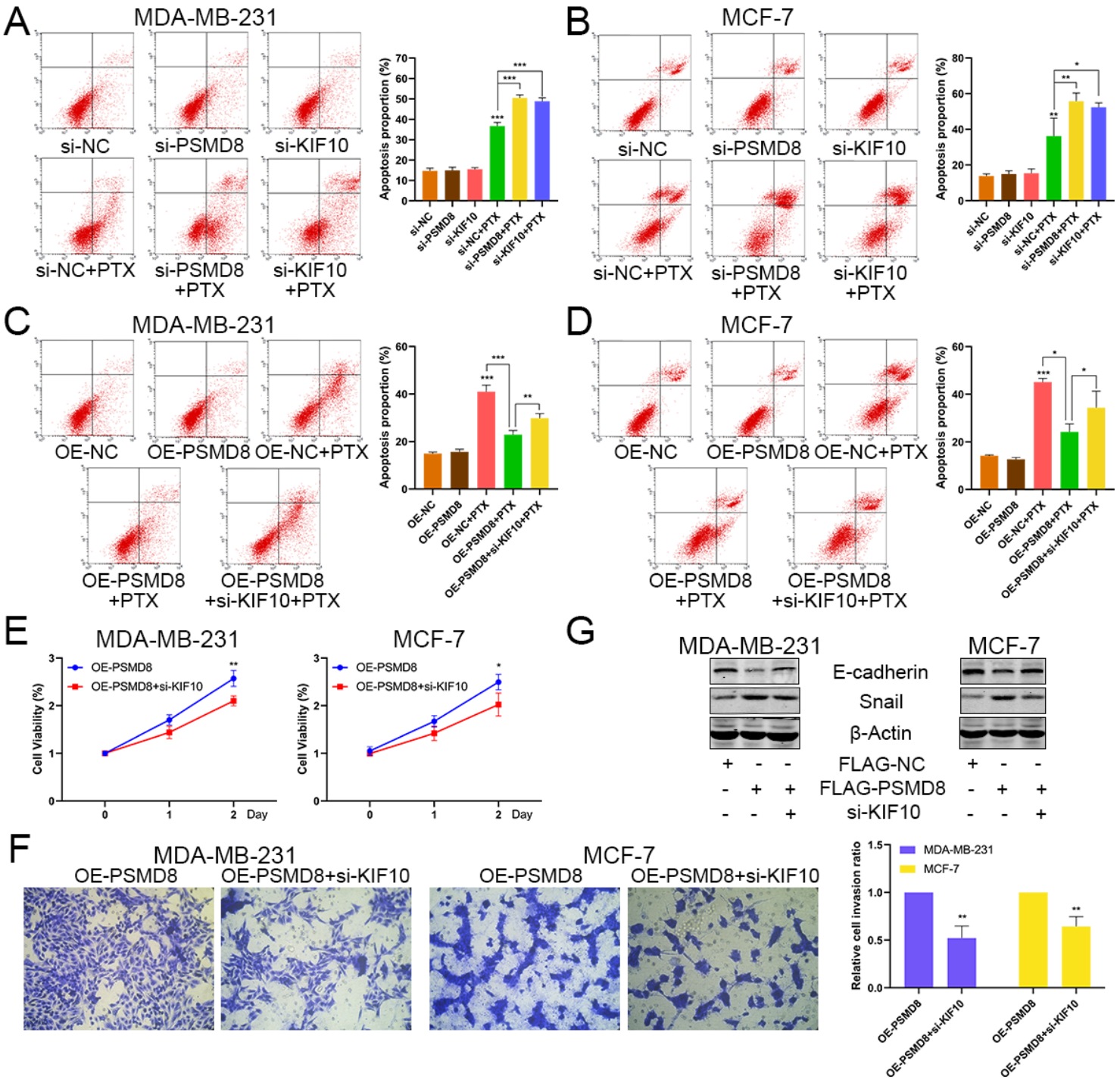

Figure 8

PSMD8/KIF10 axis promoted BC progression in vitro. (A-B) FCM in PSMD8KD and KIF10KD cells treated with 200 nM PTX for 24 h. (C-D) FCM in PSMD8OE+KIF10KD cells treated with 200 nM PTX for 24 h. (E) CCK8 assay performed in PSMD8OE+KIF10KD cells. (F) Transwell assay performed in PSMD8OE+KIF10KD cells. (magnification 200×). (G) EMT-related protein levels in PSMD8OE+KIF10KD cells. The values are presented as the means ± SD from three independent experiments. *p<0.05, **p<0.01, and ***p<0.001 compared with the corresponding group.

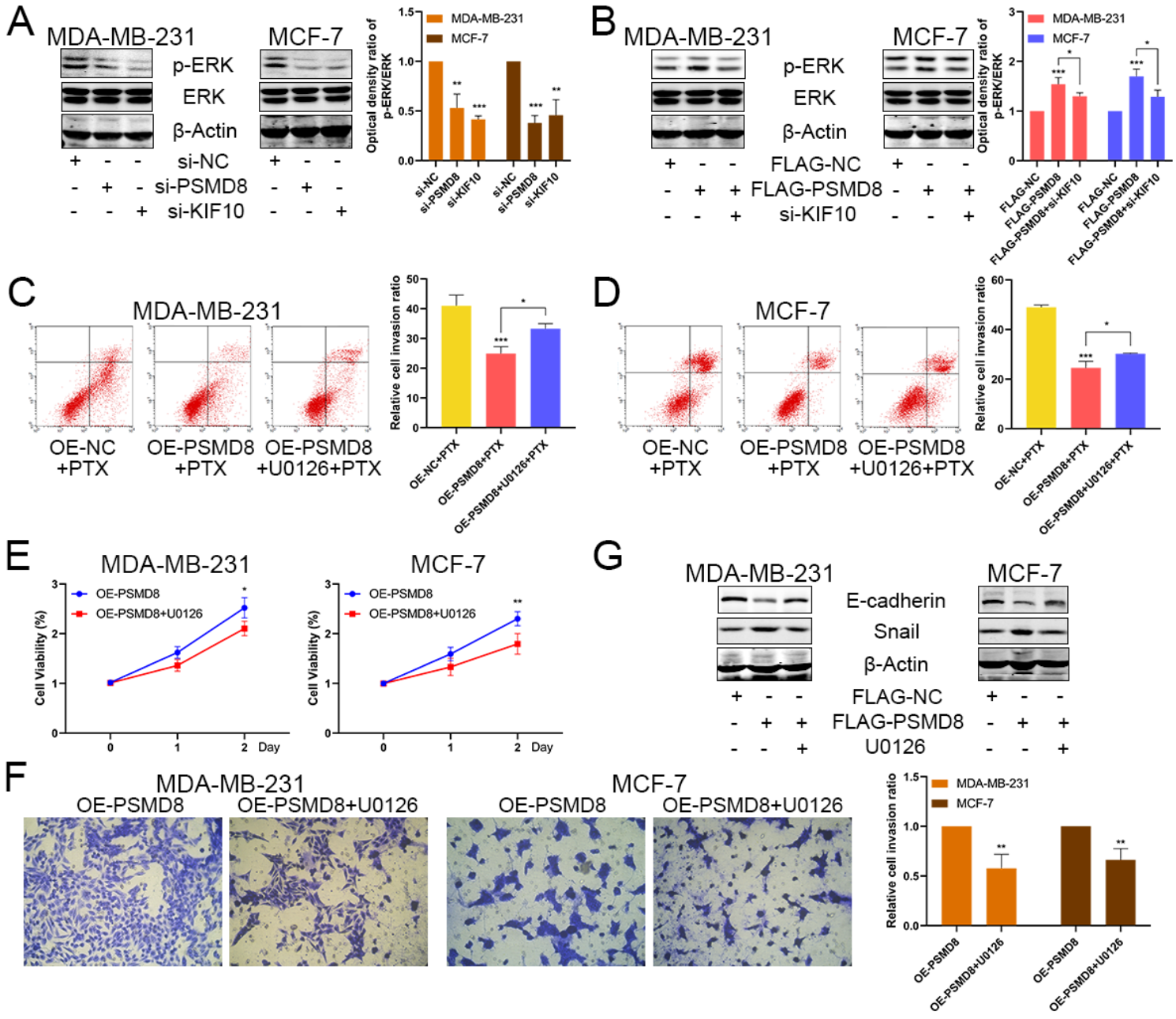

Figure 9

The PSMD8/KIF10 axis regulated BC progression, EMT and chemosensitivity via the ERK pathway. (A) p-ERK and ERK levels measured by WB in PSMD8KD and KIF10KD cells, respectively. (B) p-ERK and ERK levels measured by WB in PSMD8OE+KIF10KD cells. (C-D) PSMD8OE cells were treated with 20 μM U0126 for 24 h. Then, 200 nM PTX was added for 24 h of treatment. FCM were subsequently performed to detect cell apoptosis. (E) CCK-8 assay performed in PSMD8OE cells treated with 20 μM U0126 for 24 h. (F) Transwell assay performed in PSMD8OE cells treated with 20 μM U0126 for 24 h. (magnification 200×). (G) Cells were treated as above. WB was performed to detect the protein levels of E-cad and snail. The values are presented as the means ± SD from three independent experiments. *p<0.05, **p<0.01, and ***p<0.001 compared with the corresponding group.

Supplementary Files

This is a list of supplementary files associated with this preprint. Click to download.

- supplementarytable1.docx